ECCOMAS Thematic Conference on Computational Methods
in Structural Dynamics and Earthquake Engineering
M. Papadrakakis, D.C. Charmpis, N.D. Lagaros, Y. Tsompanakis (eds.)
Rethymno, Crete, Greece, 13–16 June 2007

CLOSED-LOOP FEEDBACK MODEL OF CHATTER IN A SHAPING OPERATION

Ayman A. El-Badawy[1], and Tarek N. Nasr El-Deen[2]

[1] Department of Engineering Mechanics, Faculty of Engineering & Materials Science
The German University in Cairo, New Cairo City, Al-Tagamoa Al Khames, Egypt
e-mail: ayman.elbadawy@guc.edu.eg

[2] Mechanical Engineering Department
Faculty of Engineering, Al-Azhar University, Nasr City, Cairo, Egypt
tareknasr_m@hotmail.com

Keywords: Regenerative Chatter, Closed-loop, Machining.

Abstract. *The motivation of the work is twofold: (a) understand the physics behind regenerative chatter while presenting some experimental results to demonstrate the problem on a shaping operation, (b) develop a closed-loop time-delayed displacement feedback mathematical model that represent the chatter phenomenon. The model is then used to investigate certain combinations of cutting force and spindle speed that leads the feedback loop to become unstable. The root locus and bode-plot techniques are used to complement the physics with a control engineering perspective. Then, the stability lobe diagrams are compared with root locus and bode-plots of the system in order to validate the feedback model. Finally, instabilities due to structural and delay poles are identified and illustrated.*

1 INTRODUCTION

One of the limiting characteristics of precision manufacturing is vibration. The force acting on a vibrating system is usually external to the system and independent of the motion. However, there are systems in which the exciting force is a function of the motion itself. Such systems are called self-excited vibrating systems. Since the motion itself produces the exciting force. The self-excited phenomenon within a manufacturing process is a cause of these vibrations. Rigid body motion of tool and workpiece can excite one or more flexible modes of the tool during machining causing precision difficulties. An example of such phenomenon is chatter which can be developed between the tool and the workpiece of a machining process. Chatter is the intermittent separation of the tool from the workpiece while cutting due to the interaction of cutting forces that change with both time and dynamic stiffness of the machine. Clearly, this vibration occurrence reduces quality and can even result in structural failure. So, the main advantage of the chatter prediction through the stability charts is the metal removal rate maximization, at the same time avoiding the adverse effects of chatter vibrations like the poor surface finish, noise and breakage of tools.

The explanation of machine-tool vibration was first given by Tobias [1] as “chip-thickness variation effect” or “regenerative effect”. The later one has become the most commonly accepted explanation for machine tool chatter. Figure 1 shows the cutting force variation due to the wavy work-piece surface cut during the previous revolution. The corresponding mathematical models are delay-differential equations (DDE). Stability properties can be predicted through the investigation of both DDEs and experimental conditions. Many researchers [2-12] provided the development of stability lobe diagrams (SLD) that compactly represent the stability information as a function of the control parameters (i.e., spindle speed and depth of cut). An important result from these analyses is the ability to identify stable cutting regions in which larger metal removal rates could be obtained by cutting at higher spindle speeds.

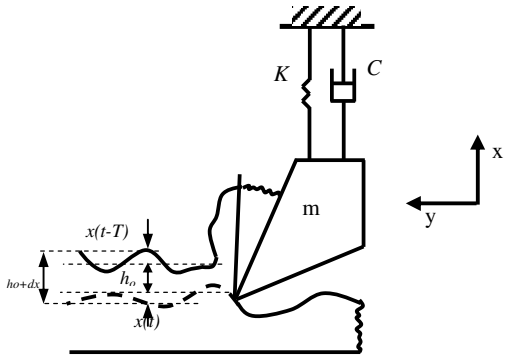

Figure 1: The Regeneration Process

Theory of chatter can be explained through different point of views; Bhattacharyya [13] summarized the different theories and models into four main groups: I) Velocity principle, II) Regenerative principle, III) Mode coupling theory and IV) Phase lag theory.

Insperger et al [2] identified the chatter frequencies in milling processes, both analytically and experimentally. Frequency diagrams are constructed analytically and attached to the stability charts of mechanical models of high-speed milling. The corresponding quasi periodic solutions of the governing time-periodic delay-differential equations are also identified with some milling experiments in the case of highly intermittent cutting.

A chatter stability study and its reasoning based on root locus plot analysis of time delayed systems is presented by Olgac and Hosek [3].

The high speed milling process is modeled by Faassen et al [4]. The experiments showed that both the material properties and the machine dynamics are dependent on the spindle speed. Furthermore, a set of linear non-autonomous delay-differential-equations for the prediction of the chatter boundaries is proposed and applied in order to predict the chatter boundaries as a function of process parameters, such as spindle speed and depth-of-cut. The modeled chatter boundaries are compared to the experimental results in order to validate the model and the stability analysis.

Kovačić [5] investigated a model of chatter vibrations in metal cutting. The model of the system is based on the predictive machine theory of shear zone model. Since the dynamic cutting force is strongly influenced by the variations of cutting parameters, the variations of rake angle and shear angle during feeding rate change are considered, and proposed a modified nonlinear model of cutting force and, consequently, nonlinear analytical model of chatter.

A method based on the approximation of the delayed term in a milling operation presented by Insperger and Stépán [6]. The technique is used for determining the stability conditions of delayed differential equations with time periodic coefficient.

L. Le-Ngoc [7] introduced the use of the frequency as an intermediary term to derive analytically the delay-dependent stability criteria for two types of time-delayed displacement feedback single-degree-of-freedom (s.d.o.f.) systems: the regenerative chatter problem, and a general linear time-delayed displacement feedback system.

In this work, some experimental chatter signatures are shown from a shaping operation. To model regenerative chatter dynamics, delay differential equations are developed. These equations are then presented in a closed-loop feedback model. Root locus and Bode diagrams are generated. These plots are then used to determine the type of poles (structural poles or time-delay poles) that lead to system instabilities.

2 EXPERIMENTS

2.1 Setup and modal properties

The First to model chatter, the values of the natural frequency and damping ratio of the cutting tool first transverse vibration mode need to be determined. These dynamic properties were identified using impact testing. A schematic representation of the experimental setup is shown in Figure 2. It consists of a shaper machine, accelerometer, impulse hammer, spectrum analyzer and a PC.

The absolute value of the measured frequency response function is depicted in Figure 3 (mean of 10 measurements). From this frequency response function, the natural frequency and damping ratio of the first bending mode of tool were found to be 285 Hz and 0.091 respectively.

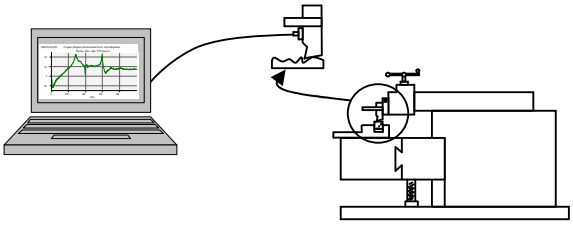

Figure 2: Shaper machine, workpiece, and data acquisition system layout.

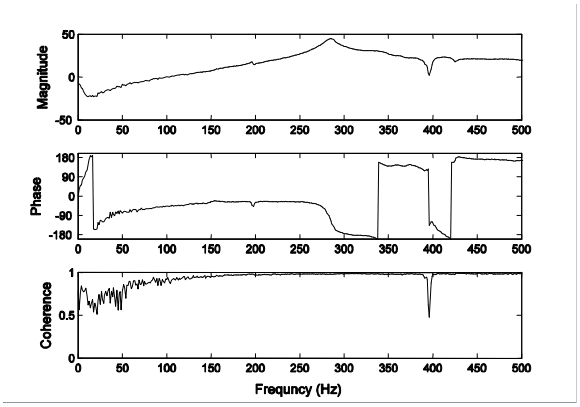

Figure 3: Frequency response function for the tool (magnitude, phase and coherence).

2.2 Chatter signature

Different cutting conditions were applied by changing the shaper speed and depth of cut. The available speeds were 12, 18, 26, 35 and 50 strokes per minute and for each speed, different values (0.05, 0.10, 0.15… 1.00 mm) for the depth of cut (DOC) were used.

Power spectral density and time traces of the tool acceleration were acquired for these different cutting conditions. Figure 4 shows a sample of the tool response for depth of cut of 0.20 and 0.70 mm and 12 strokes/min cutting speed. We notice that by increasing the depth of cut from 0.20 to 0.70 mm keeping the same speed; the cutting operation passed through a stability boundary and the cutting operation became unstable.

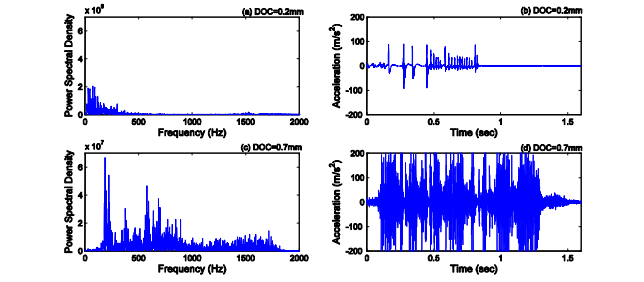

Fig. 4. Power spectral density and time traces of the tool acceleration for (a, b) DOC=0.20mm, (c, d) DOC=0.70mm and 12 strokes/min cutting speed.

3 MODELING AND STABILITY ANALYSIS

3.1 Mathematical modeling

In this work, we assume that chatter is associated with a single mode of vibration of the tool and therefore can be modeled as a single degree of freedom (SDOF) system. The cutting force is assumed to be proportional to the chip thickness, so it is dependent on previous cutting conditions. The fluctuating cutting force, *df* is given by

$$df = -K\left(x(t) - x(t-T)\right) \tag{1}$$

where K is a constant called cutting force factor, $x(t)$ is the time-dependent displacement of the tool from the equilibrium position. $x(t-T)$ is the displacement of the tool at time t-T, where T is the time delay.

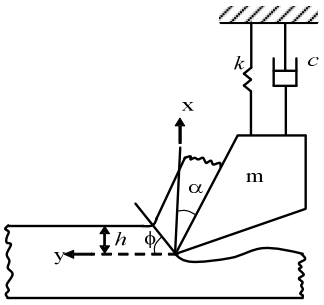

Figure 5: Single degree of freedom mechanical model

Figure 5 shows a SDOF mechanical model of the regenerative machine tool vibration in the case of the so-called orthogonal cutting (*h* denotes chip thickness; ϕ is the shear angle and α is the rake angle).

The SDOF equation of motion of the tool is given as

$$m\ddot{x}(t) + c\dot{x}(t) + kx(t) = -K\left(x(t) - x(t-T)\right) \tag{2}$$

where *m, c,* and *k* are the equivalent mass, damping coefficient and stiffness of the tool respectively. Equation (2) can be expressed as

$$\ddot{x}(t) + 2\zeta\omega_n\dot{x}(t) + \omega_n^2 x(t) = -Y\omega_n^2\left(x(t) - x(t-T)\right) \tag{3}$$

where $\omega_n = \sqrt{k/m}$ is the natural angular frequency of the undamped free oscillating system, and $\zeta = c/(2m\omega_n)$ is called the relative damping factor and $Y=K/k$ is the non-dimensional gain factor.

3.2 Stability analysis

The solution of (3) has the form $x=Ae^{-st}$, where *s* is the complex characteristic value ($s=\sigma+i\omega$) where σ is the decay rate and ω is the angular frequency. The dynamic characteristics of the response are represented by the decay rate σ, and angular velocity ω. The system is stable if σ is negative and unstable otherwise. The stability boundary condition is $\sigma=0$.

Substituting *x* into (3) gives the following characteristic equation:

$$s^2 + 2\zeta\omega_n s + \omega_n^2 + Y\,\omega_n^2\left(1 - e^{-sT}\right) = 0 \tag{4}$$

then substituting for *s* in (4) by σ and ω and separating the real and imaginary parts gives

$$-\omega^2 + \omega_n^2 + Y\,\omega_n^2\left(1 - \cos\omega T\right) = 0 \tag{5a}$$

$$2\zeta\omega_n\omega + Y\,\omega_n^2 \sin\omega T = 0 \tag{5b}$$

By introducing the non-dimensional terms $W=\omega/\omega_n$, and $\tau=T\omega_n$, the above equations can be written in non-dimensional form as

$$\begin{aligned} -W^2 + 1 + Y\,(1 - \cos W\tau) &= 0 \\ 2\zeta W + Y\,\sin W\tau &= 0 \end{aligned} \tag{6a, b}$$

These two simultaneous equations represent the dynamics of the tool, subjected to a cutting force of amplitude *Y*, delayed by time τ, and with system damping characteristics ζ.

Equations (6a, 6b) may be rearranged to produce two equations, explicitly expressing Y in terms of W and ζ and τ in terms of W and ζ. Rearranging (6b) gives

$$Y = \frac{-2\zeta W}{\sin W\tau} \tag{7}$$

and substituting it into (6a) gives

$$-W^2 + 1 - 2\zeta W \tan\frac{W\tau}{2} = 0 \tag{8}$$

So,

$$\tau = \frac{2}{W}\left(\tan^{-1}\left(\frac{1-W^2}{2\zeta W}\right) + n\pi\right), \qquad n = 0,1,2,.....,\infty \tag{9}$$

Substituting (9) into (7) to eliminate τ, and simplifying to find an explicit expression for Y in terms of W and ζ

$$Y = \frac{-\left(1-W^2\right)^2 - \left(2\zeta W\right)^2}{2\left(1-W^2\right)} \tag{10}$$

The damping ratio ζ may be assumed to be constant for a particular system. Therefore (9, 10) represent a set of parametric equations for the stability boundary in terms of τ and Y.

For zero damping ζ=0, Y is simply a parabola with a discontinuity at W=1 (Fig. 6a). As damping increases, the discontinuity at W=1 becomes more pronounced (Fig. 6b). This curve represents the stability boundary for the feedback gain factor Y as a function of frequency W for a given damping ratio ζ. From physics it is known that the feedback gain factor Y can be only a positive value. So, the negative lobe in Figures 6a and 6b are for mathematical representation only while the upper lobe represents one of the stability lobes in Fig. 8. The regions of instability can be easily determined using (5b). if the *LHS* of (5b) is negative then the system is stable and unstable otherwise.

The minimum point of instability region can be found by differentiating (10) with respect to W and equating to zero to give

$$\frac{dY}{dW} = \frac{W\left(W^4 - 2W^2 + 1 - 4\zeta^2\right)}{\left(1-W^2\right)^2} \tag{11}$$

There are five roots for this equation: they are $W = 0$, $W = \pm\sqrt{1 \pm 2\zeta}$. Root $W = \sqrt{1+2\zeta}$ relates to the minimum of the instability region, whereas $W = \sqrt{1-2\zeta}$ is the maximum of the instability region for $W < 1$.

The relationship between τ and W is represented by the infinite number of curves produced by the periodic nature of the transcendental (9). Figure 7a shows the curves for n=0, 1, 2, 3 and 4 for ζ=0.1. Figure 7b shows the relationship between X and W, where X is the repeat of the delayed signal, Ω in a non-dimensional form $X = \Omega/\omega_n = 2\pi/\tau$. Fig. 8 shows the standard stability chart for regenerative chatter problem. This figure shows that the time delay independent stability criterion is $Y < 2\zeta(1+\zeta)$. With the assist of Figures 7-8, the stability parameters condition (W and τ) can be determined. For example, from Figure 8 we have for the

2nd lobe ($n=2$), the minimum stability limit is $X = 0.626$. From Figure 7b, this value of X leads to $W = 1.1$ for the same stability lobe. Using this transformation, we can plot the whole stability diagram as a function of the cutting speed instead of chatter frequency. This leads to a more meaningful stability diagram since the cutting speed is a control parameter. Finally, we plug this value of W into Figure 7a to determine the critical delay time value. This value is then used later to draw the root locus and Bode diagrams.

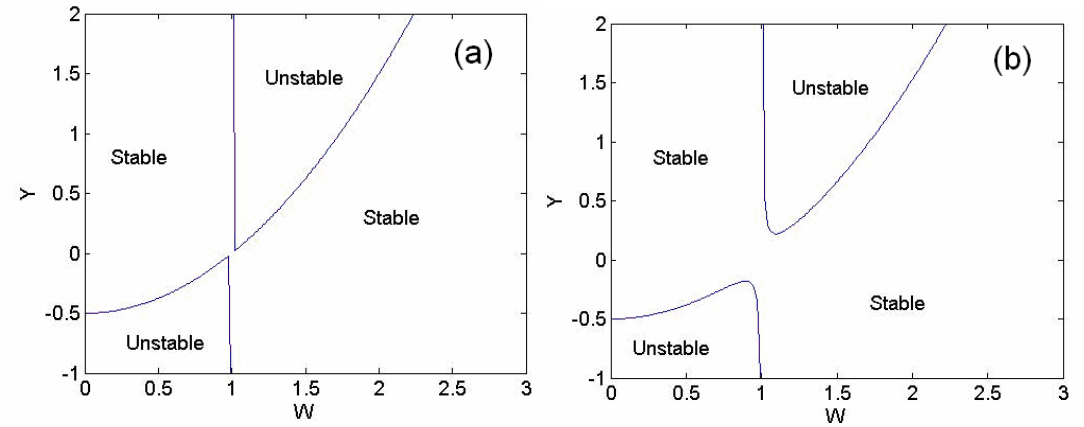

Figure 6: Stability chart for regenerative feedback system on a force Y versus chatter frequency W : a) $\zeta = 0$, b) $\zeta = 0.1$

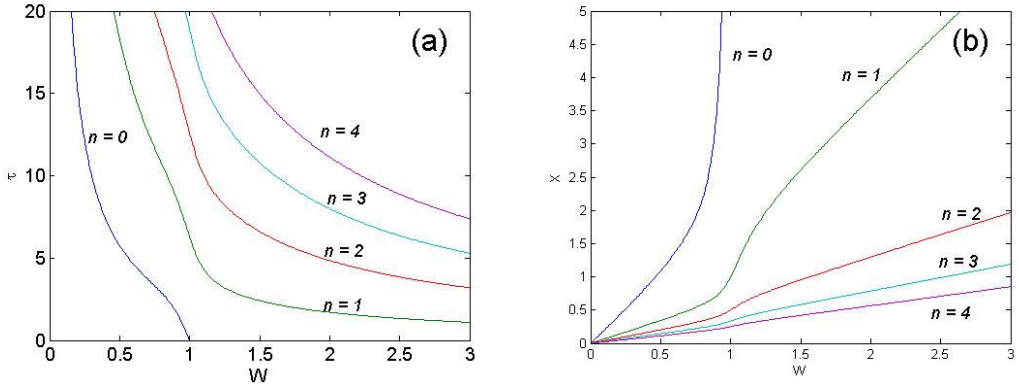

Figure 7: Relationship between chatter frequency W and a) time delay τ, b) repeat frequency X ($\zeta = 0.1$, n = 0, 1, 2, 3, 4)

4 CLOSED-LOOP FEEDBACK MODEL

Referring to (Figure 1) and assuming the tool to be flexible only in the x-direction, the uncut chip thickness at any instant is given by

$$h(t) = h_o(t) + x(t - T) - x(t) \tag{12}$$

Assuming that the cutting force is proportional to the chip thickness, as previously shown in (2), then the cutting force F_c in the x-direction is equal to

$$F_c = Kh(t) = K\left(h_o(t) + x(t - T) - x(t)\right) \tag{13}$$

Under certain combination of cutting conditions, the feedback becomes unstable, leading to chatter. The dynamic equation of motion in the x direction is

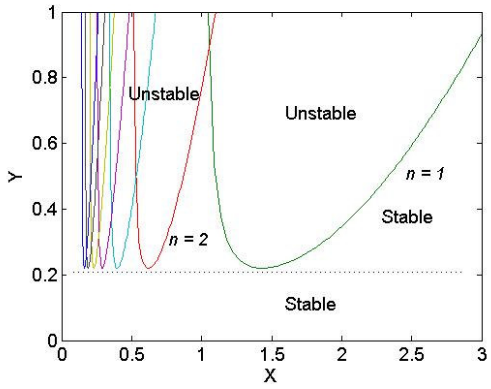

Figure 8: Stability chart for feedback system on a force Y versus repeat frequency X (ζ = 0.1, n = 1 – 7)

$$\ddot{x}(t)+2\zeta\omega_n\dot{x}(t)+\omega_n^2 x(t)=F_c(1/m) \tag{14}$$

Equations (12, 13 and 14) represent the regenerative cutting model in the time domain. Applying Laplace transform to these equations yield

$$h(s)=h_o(s)+x(s)\left(e^{-sT}-1\right) \tag{15}$$

$$F_c(s)=Kh(s) \tag{16}$$

$$x(s)=G(s)F_c(s) \tag{17}$$

Defining the machine tool transfer function between the applied force F and displacement x as G(s), we have $\frac{x(s)}{F_c(s)}=G(s)=\frac{(1/m)}{s^2+2\zeta\omega_n s+\omega_n^2}$.

Figure 9 represents the closed-loop feedback diagram for regenerative chatter. In this figure h_o is the desired feed of the tool and h is the total chip thickness.

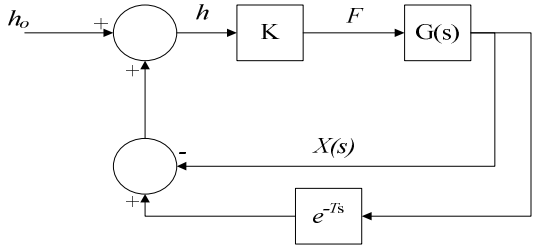

Figure 9: Closed-loop representation of regenerative chatter

Rearranging (15, 16 and 17) we get

$$\frac{h(s)}{h_o(s)}=\frac{1}{1+KG(s)\left(1-e^{-sT}\right)} \tag{18}$$

To model time delay effects within the context of continuous-time systems a padé [14] approximant is used

$$e^{-Ts} \cong \frac{1-\frac{Ts}{2}+\frac{(Ts)^2}{8}-\frac{(Ts)^3}{48}+\cdots}{1+\frac{Ts}{2}+\frac{(Ts)^2}{8}+\frac{(Ts)^3}{48}+\cdots} \tag{19}$$

Root locus plots of various delay times is shown in Figure 10. We found that for very small time delay (i.e. $\tau \to 0$) its effect on system stability can be ignored because poles due to time delay are on the extremely left side of the imaginary axis (Figure 10a). With increasing the delay time values (Figure 10b,c), the delay roots approach the imaginary axis and cross it. Traditional techniques of chatter analysis generally recognize that instability arises from the structural mode of the system. However, it can be said from Figure 10, that for certain spindle speeds, there is always a possibility that the roots due to the delay may cross over to the right side of the imaginary axis before a structural pole does.

Realizing that the root locus and bode plots are drawn for a specific delay time, this specific diagram point up the value of the chatter frequency. These values of the chatter frequency and time delay together with a trial value of stability lobe number (n) guided from Fig. 7a are used to determine a chatter frequency X from Figure 7b. If this X value agrees with the one determined from the root locus diagram, then the stability lobe number is the correct one; otherwise, repeat for a different n value until X agrees between the mathematical model and the closed-loop feedback model.

Knowing the confirmed value of X together with the determined value of n, the corresponding value of $W\left(\omega/\omega_n\right)$ from Figure 7b is determined. Having now the value of ω and the value of GM obtained from the Bode plot, a point on the stability chart can be located. Thus we can relate the closed-loop feedback model with mathematical model. This can be important when designing a compensator and correlating the behavior of the controlled system back to the stability charts. Converged results is achieved when eighteen terms in (19) was used. Figure 11 shows the stability chart for both cases (a) mathematical model and (b) closed-loop feedback model.

Using the root locus diagrams, the value of the critical speed where the delay poles start crossing the imaginary axis is determined. This value is then used in the stability chart (Figure 12) to separate the two regions of stability lobes, the one due to structural poles and the one due to delay poles.

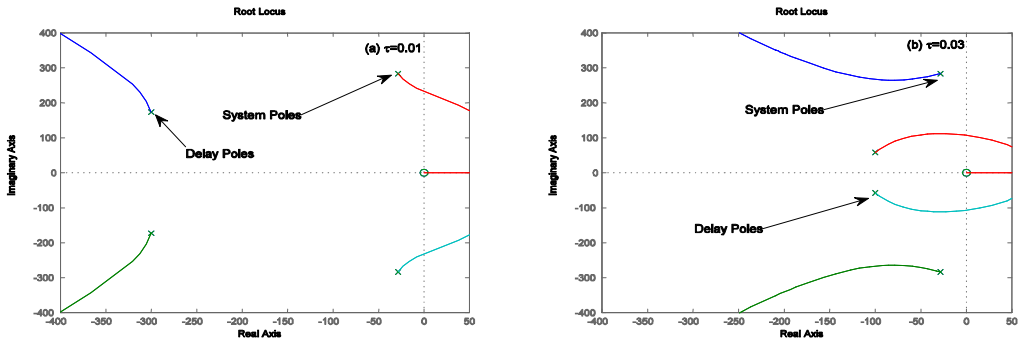

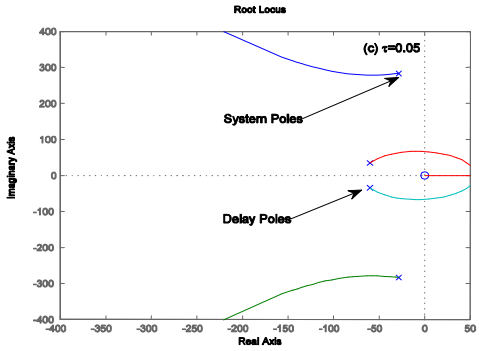

Figure 10: Root Locus Plots for (a) $\tau = 0.01$, (b) $\tau = 0.03$ and (c) $\tau = 0.05$

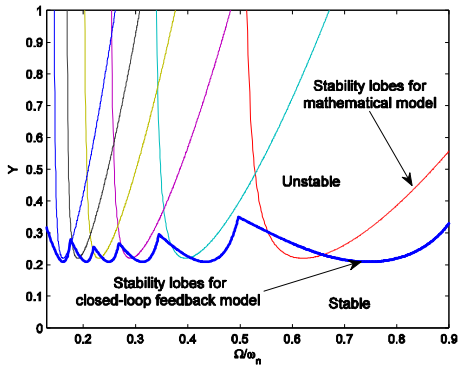

Figure 11: Stability Chart (a) mathematical model and (b) closed-loop feedback model

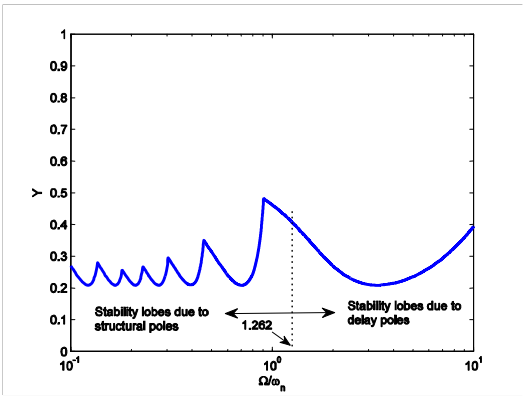

Figure 12: Stability lobe diagram obtained from closed-loop feedback model

Bode plots for the same time delay conditions are also shown in Figure 13. Table 1 presents the critical spindle speeds as well as the gain margins (K) for instability to occur. It is clear from the table that increasing the delay time increases the value of the gain margin. This is expected since the repeat frequency is the reciprocal of the delay time, and as the repeat frequency decreases, the waviness in the surface decreases leading to a better surface finish, thus higher GM for instability. It is worth noting that unlike the root locus, plotting the Bode diagram will not help in determining the type of pole that will lead to instability.

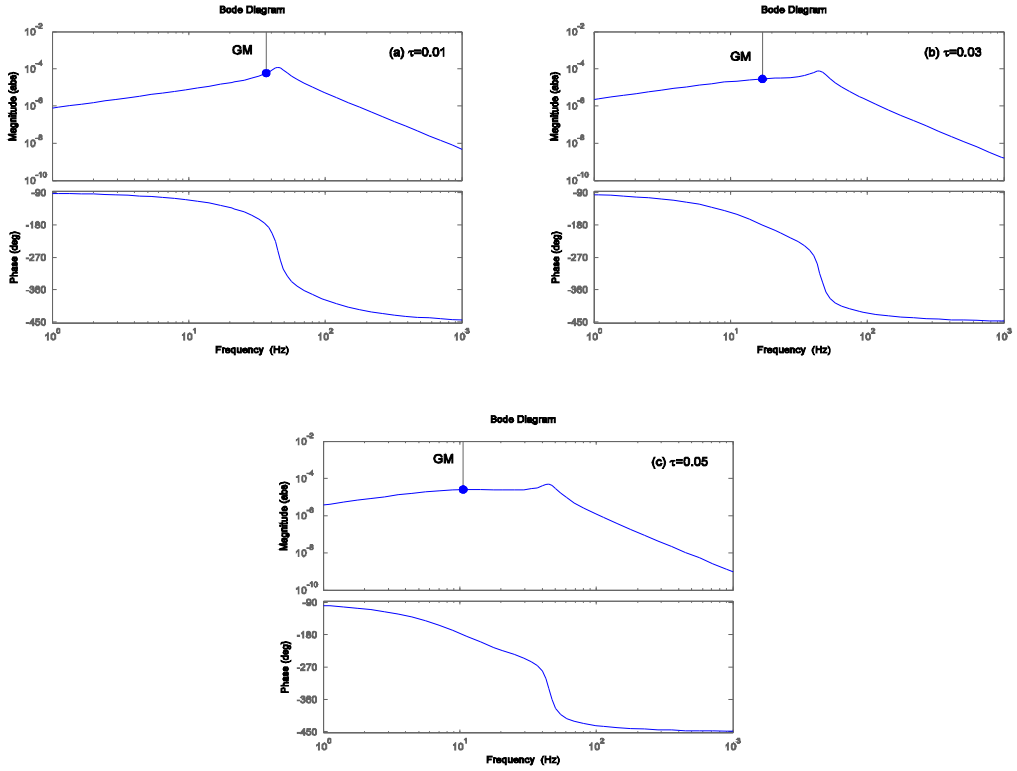

Figure 13: Bode Plots for (a) $\tau = 0.01$, (b) $\tau = 0.03$ and (c) $\tau = 0.05$

Delay Time (τ)	Bode Plot Results	
	$\omega_{cr.}$ (rad/s)	Gain Margin (K)
0.01	231	17000
0.03	106.8	35100
0.05	66.6	38500

Table 1: Bode plots results for different time delays

5 CONCLUSIONS

- Some experimental chatter signatures were illustrated for a shaping operation.
- Regenerative chatter dynamics was modeled using delay differential equations.
- The DDE equations were then correlated to a closed-loop feedback model.
- Root locus and Bode diagrams were generated.
- Root locus and Bode plots were then used to determine the type of poles (structural poles or time-delay poles) that lead to system instabilities.

REFERENCES

[1] S.A. Tobias, *Machine Tool Vibration*, Blackie & Son Limited, 1965.

[2] T. Insperger, G. Stépán, P.V. Bayly, B.P. Mann, *Multiple Chatter Frequencies in Milling Processes*. *Journal of Sound and Vibration*, **262**, 333-345, 2003.

[3] N. Olgac and M. Hosek, A New Perspective and Analysis for Regenerative Machine Tool Chatter. *International Journal of Machine Tools & Manufacture*, **38**, 783–798, 1998.

[4] R. Faassen, N. van de Wouw, J.A.J. Oosterling, H. Nijmeijer, Prediction of Regenerative Chatter by Modeling and Analysis of High-Speed Milling. *International Journal of Machine Tools & Manufacture*, **43**, 1437-1446, 2003.

[5] I. Kovačić, The Chatter Vibrations in Metal Cutting -Theoretical Approach. *University of NIŠ, The scientific journal FACTA UNIVERSITATIS, Series: Mechanical Engineering*, **1**, 581- 593, 1998.

[6] T. Insperger, G. Stépán, Stability of the Milling Process. *Periodica Polytechnica Ser. Mech. Eng.*, **44**, 47–57, 2000.

[7] L. Le-Ngoc, Simple Stability Analyses of a Regenerative Chatter Problem and of a Time-Delayed Displacement Feedback SDOF System. *Journal of Sound and Vibration*, **258**, 373-384, 2002.

[8] N. Wagner, L. Gaul, Eigenpath Analysis of Transcendental Two-Parameter Eigenvalue Problems. *European Congress on Computational Methods in Applied Sciences and Engineering (ECCOMA)*, 2004.

[9] P. Wahi , A. Chatterjee, Regenerative Tool Chatter Near a Codimension 2 Hopf Point Using Multiple Scales. *Nonlinear Dynamics*, **40**, 323–338, 2005.

[10] R. Szalai, G. Stépán, Lobes and lenses in the stability chart of interrupted turning, *accepted for ASME Journal of Computational and Nonlinear Dynamics*, 2006.

[11] B.P. Mann, N.K. Garg, K.A. Young, A.M. Helvey, Milling Bifurcations from Structural Asymmetry and Nonlinear Regeneration. *Nonlinear Dynamics*, **42**, 319–337, 2005.

[12] M. Fofana, P. Ryba, Parametric Stability of Non-Linear Time Delay Equations. *International Journal of Non-Linear Mechanics*, **39**, 79-91, 2004.

[13] A. Bhattachryya, *Metal Cutting – Theory and Practice*, New Central Book Agency, Calcutta, 2000.

[14] K. Ogata, *Modern Control Engineering*, Prentice Hall, 2002.